Clim. Past, 12, 439–454, 2016
www.clim-past.net/12/439/2016/
doi:10.5194/cp-12-439-2016

Climate of the Past
Open Access
EGU

Fossil plant stomata indicate decreasing atmospheric CO_2 prior to the Eocene–Oligocene boundary

Margret Steinthorsdottir[1], Amanda S. Porter[2], Aidan Holohan[2], Lutz Kunzmann[3], Margaret Collinson[4], and Jennifer C. McElwain[2]

[1]Department of Geological Sciences and Bolin Centre for Climate Research, Stockholm University, 106 91 Stockholm, Sweden
[2]School of Biology and Environmental Science, Earth Institute, University College Dublin, Dublin 4, Ireland
[3]Museum of Mineralogy and Geology, Senckenberg Natural History Collections Dresden, Dresden, Germany
[4]Department of Earth Sciences, Royal Holloway University of London, Egham, Surrey, UK

Correspondence to: Margret Steinthorsdottir (margret.steinthorsdottir@geo.su.se)

Received: 2 October 2015 – Published in Clim. Past Discuss.: 26 October 2015
Revised: 25 January 2016 – Accepted: 15 February 2016 – Published: 25 February 2016

Abstract. A unique stratigraphic sequence of fossil leaves of *Eotrigonobalanus furcinervis* (extinct trees of the beech family, Fagaceae) from central Germany has been used to derive an atmospheric pCO_2 record with multiple data points spanning the late middle to late Eocene, two sampling levels which may be earliest Oligocene, and two samples from later in the Oligocene. Using the inverse relationship between the density of stomata and pCO_2, we show that pCO_2 decreased continuously from the late middle to late Eocene, reaching a relatively stable low value before the end of the Eocene. Based on the subsequent records, pCO_2 in parts of the Oligocene was similar to latest Eocene values. These results suggest that a decrease in pCO_2 preceded the large shift in marine oxygen isotope records that characterizes the Eocene–Oligocene transition and that when a certain threshold of pCO_2 change was crossed, the cumulative effects of this and other factors resulted in rapid temperature decline, ice build up on Antarctica and hence a change of climate mode.

1 Introduction

1.1 The role of pCO_2 in Cenozoic climate

The Cenozoic era is characterized by large climatic variations, including the fundamentally important transition from an ice-free "greenhouse" planet to the modern "icehouse" planet with polar glaciations. This climatic transition is generally thought to have been driven primarily by changes in pCO_2 and/or the thermal isolation of Antarctica by the opening of Southern Ocean gateways (DeConto and Pollard, 2003; Zachos et al., 2008; Hansen et al., 2013; Hren et al., 2013; Goldner et al., 2014; Inglis et al., 2015). However, the full extent of the role of pCO_2 in Cenozoic climate change remains unresolved. The most detailed Cenozoic temperature and pCO_2 records are derived from marine isotope proxies (e.g. Foster et al., 2012; Pagani et al., 2011; Pearson et al., 2009; Zachos et al., 2001, 2008). Isotope records, however, may be influenced by a variety of taphonomic and diagenetic biases (see Coxall and Pearson (2007) for review; and Pagani et al., 2011), which can obscure the climatic signal, and thus need independent evaluation by separate proxy records (Beerling and Royer, 2011).

Eocene temperatures were globally much higher than today, leading to a weakened Equator-to-pole temperature gradient and muted seasonal cycle compared to today – the so-called "Eocene equable climate problem" (Sloan and Barron, 1992; Huber and Caballero, 2011). Climate modelling has been able to reconstruct this climatic pattern only with excessively high pCO_2 levels ($\sim$ 4500 ppm: Huber and Caballero, 2011), but such elevated pCO_2 atmospheres do not agree with most proxy records. It has therefore been speculated that Eocene climate sensitivity was elevated compared to today and/or that other forcing in addition to high pCO_2 was involved (Caballero and Huber, 2013; Hansen et al., 2013).

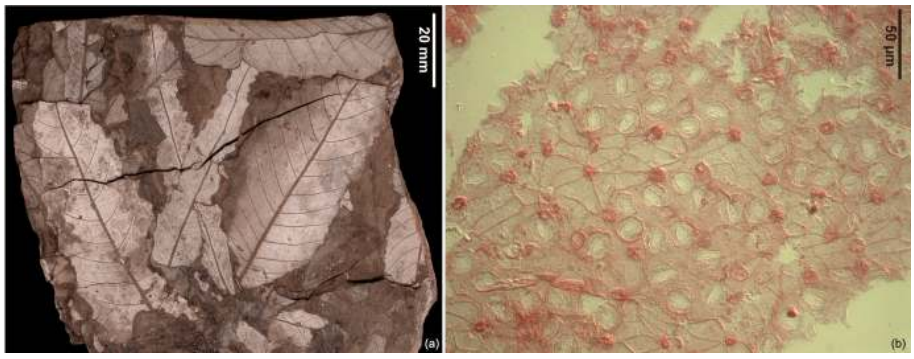

Figure 1. *Eotrigonobalanus furcinervis* (Rossmässler, 1840; Kvaček and Walther, 1989): **(a)** mass occurrence of leaves in lignite, Schleenhain opencast mine, Saxony, Germany, site Schleenhain 2, Borna Formation, Bruckdorf Member, late Eocene (Priabonian), SPP zone 18o, MMG PB SchleOE 535; **(b)** abaxial leaf cuticle with stomata and trichome bases, Schleenhain opencast mine, Saxony, Germany, site Schleenhain 4, Böhlen Formation, Gröbers Member, earliest Oligocene (Rupelian), SPP zone 20A/B, slide MMG PB SchleMO 11/05 from leaf SchleMO 556/2.

In order to solve this enigma reliable multiple proxy records of pCO_2 are of paramount importance.

The fundamental climatic reorganization that occurred close to the Eocene–Oligocene boundary (33.8 Ma), often referred to as the Eocene–Oligocene transition (EOT, 34–33.5 Ma), had drastic consequences for biological systems. These included both terrestrial and marine faunal and floral extinctions accompanied by evolutionary turnover (Prothero, 1994; Coxall and Pearson, 2007; Sheldon et al., 2009: Kunzmann, 2012; Kvaček et al., 2014), although vegetation changes in the European terrestrial record appear to be less dramatic and more gradual (Kvaček et al., 2014; Kunzmann et al., 2015). General circulation models of Palaeogene climate have shown that continuously declining pCO_2, amplified by Milankovitch forcing and ice-albedo feedbacks, could cause significant temperature reduction. This could result in a permanent continental Antarctic ice-sheet once a critical pCO_2 threshold, generally considered to be < 700 ppm is crossed (e.g. DeConto and Pollard, 2003; Coxall et al., 2005; Pollard and DeConto, 2005; Zachos and Kump, 2005; Pagani et al., 2011; Hansen et al., 2013). Modelling studies thus indicate that lowering of pCO_2 may have been the primary forcer of this cooling transition (DeConto and Pollard, 2003; DeConto et al., 2008). However, detailed estimates for pCO_2 for the Eocene and the Oligocene are highly variable and sometimes contradictory or showing unexpected relationships with palaeo-temperature proxy records (see Pagani et al., 2005). For example, comparing the pCO_2 record of Pearson et al. (2009: Fig. 1), which is based on measurements of boron isotopes in planktonic foraminifera, and the benthic foraminifera oxygen isotope ($\delta^{18}O$) compilations of Zachos et al. (2008), it is evident that in the late Eocene $\delta^{18}O$-inferred deep ocean cooling coincided with decreasing pCO_2. In contrast, there is little evidence of warming in the early Oligocene, despite a surprising initial large increase in pCO_2. Overall, the pCO_2 and O isotope-based temperature records seem to be (largely) coupled in the Eocene, but decoupled in the Oligocene. Pagani et al. (2011) on the other hand recently published compiled alkenone-based pCO_2 records and found declining pCO_2 before and during the Antarctic glaciation (EOT and earliest Oligocene) (Pagani et al., 2011: Fig. 4), supporting the role of pCO_2 as the primary forcing agent of Antarctic glaciation, consistent with model-derived thresholds. A compounding factor of these discrepancies is that the influence of temperature on ice sheet volume is unconstrained and the influence of temperature versus ice volume on the $\delta^{18}O$ record is unresolved, with no proxy identified to isolate ice sheet volume changes, complicating further the interpretation of the climate proxy data sets. Independent proxy records of E–O pCO_2 are therefore desirable and may support one or the other of the major prevailing scenarios outlined above, or provide alternative information on Cenozoic climate change.

One of the four proxies that have been identified as being particularly useful for Cenozoic pCO_2 reconstructions by the Intergovernmental Panel on Climate Change (initially reported in the Fourth IPCC Report; IPCC, 2007) is the terrestrial proxy based on stomatal densities of fossil plants. Previous studies using the stomatal proxy method of pCO_2 reconstructions for the part of the Cenozoic relevant here were, however, mostly of low resolution and have been inconclusive. Some suggested that pCO_2 was essentially stable at between 300 and 450 parts per million by volume (ppm) during the Eocene, Oligocene and Miocene (Royer, 2001; Royer et al., 2001; Greenwood et al., 2003; Maxbauer et al., 2014) and others suggesting distinct decrease in pCO_2 across the Eocene–Oligocene boundary (Retallack, 2001). More recent studies suggest higher and possibly rapidly decreasing pCO_2 (ranging ca. 1000–500 ppm) during the late middle Eocene (Doria et al., 2011; Grein et al., 2011). In this issue, Liu et al. report a "late Eocene" pCO_2 from a single stratigraphical level of ca. 390 ppm. However, the chronological range they

supply for their pCO_2 estimate (42.0–38.5 Ma) falls within the late Lutetian to Bartonian in the Middle Eocene, thus recording an unusually low pCO_2 estimate for this time-interval characterized by high temperatures (Liu et al., 2015). Closer to the E–O boundary, one study suggests that pCO_2 was significantly higher at the EOT than during the early Oligocene (Roth-Nebelsick et al., 2004) and others that early Oligocene to early Miocene pCO_2 was ca. 400 ppm throughout (Grein et al., 2013; Roth-Nebelsick et al., 2014).

Here we present a new stomatal proxy-based record with multiple data points spanning the late middle to late Eocene, two sampling levels that according to current available evidence are from the earliest Oligocene, and two samples from later in the Oligocene.

1.2 The stomatal proxy method of palaeo-pCO_2 reconstruction

Stomata are pores on plant leaf surfaces through which gas exchange takes place; i.e. carbon is obtained from CO_2 and at the same time water vapour and oxygen are lost by diffusion. An inverse relationship exists between the frequency of stomata and pCO_2, as established by Woodward (1987) from observations of herbarium material, showing that modern tree species have responded to the anthropogenic rise in pCO_2 by reducing their stomatal frequency significantly. The inverse relationship between stomatal frequency, recorded as "stomatal density" (SD = the number of stomata per mm^2) or "stomatal index" (SI = the percentage of stomata relative to epidermal cells), and pCO_2 has been repeatedly demonstrated for a wide variety of plant taxa from disparate geological and ecological settings from the Palaeozoic until today and is thus established as a strong proxy for palaeo-pCO_2 (e.g. Beerling et al., 1998; McElwain, 1998; Retallack, 2001; Royer et al., 2001; Kürschner et al., 2008; Steinthorsdottir et al., 2011b; 2013: Steinthorsdottir and Vajda, 2015). The increasingly close match between stomatal proxy pCO_2 results and independent proxy records, actual pCO_2 measurements and in some cases climate modelling (e.g. Finsinger and Wagner-Cremer, 2009; Foster et al., 2012; Kürschner et al., 2008; Retallack, 2001; Rundgren and Björck, 2003; Steinthorsdottir and Vajda, 2015) instils growing confidence in stomatal frequency for recording past pCO_2. Strongly supporting the validity of the stomatal proxy is also the identification of the mechanism by which plants control their stomatal densities based on atmospheric pCO_2. All plants use the enzyme carbonic anhydrase to detect pCO_2 around their leaves (Frommer, 2010; Hu et al., 2010); mature leaves (early shoots) then control stomatal development of younger leaves through long-distance signalling (Lake et al., 2002), involving the HIC gene signalling pathway (Brownlee, 2001; Gray et al., 2000).

In order to transform stomatal frequency data derived from fossil plants into palaeo-pCO_2 estimates it is usually necessary to compare stomatal data from present-day plants that are either phylogenetically related or in other ways equivalent to the fossil plants. Nearest living relatives (NLRs) should be used when possible, but when these cannot be identified for the fossil plants, nearest living equivalents (NLEs = present-day species that are of comparable ecological setting and/or structural similarity to their fossil counterpart) may be used instead (McElwain and Chaloner, 1995; Barclay et al., 2010; Steinthorsdottir et al., 2011a, b).

There are three stomatal palaeo-pCO_2 calibration methods in use. These are (i) the "stomatal ratio method" (McElwain and Chaloner, 1995; McElwain, 1998), which relies on a ratio between stomatal frequencies of fossil plants and their NLE to semi-quantify pCO_2; (ii) the "transfer function method", which relies on herbarium material and/or experimental data sets for NLR/NLE responses to calculate pCO_2 curves (e.g. Beerling and Royer, 2002); and (iii) the more recently developed taxon-independent "mechanistic gas exchange modelling" approach (e.g. Wynn, 2003; Konrad et al., 2008; Franks et al., 2014; Grein et al., 2013; Roth-Nebelsick et al., 2014) which all use measurements of stomatal density and pore size to estimate maximum theoretical gas exchange rates, together with various photosynthetic biochemical traits, and in some cases palaeoenvironmental information, to estimate palaeo-CO_2. The stomatal ratio method, which is used here, calibrates palaeo-pCO_2 based on two so-called standardizations. The first is the "modern" standardization that assumes that the ratio between past and modern pCO_2 is 1 ($RCO_2 = 1$) and is applied to young material, typically from the Quaternary. The second is the "Carboniferous" standardization that sets the ratio between past and modern pCO_2 at two times preindustrial levels of 300 ppm ($RCO_2 = 2 = 600$) (McElwain and Chaloner, 1995). Both standardizations are usually applied to fossil leaf material of Cenozoic age and older to yield minimum and maximum pCO_2 estimates and both standardizations will be used in this paper.

We have chosen not to apply the mechanistic optimization model of Konrad et al. (2008) to our study, because it has recently been shown in a modern test of the model to produce the most accurate pCO_2 estimates when used on multiple species, to derive a consensus pCO_2 estimate from their area of overlapping pCO_2 values (Grein et al., 2013), and we here study a one-species database. The optimization model produces very large and species-dependent uncertainty in pCO_2 estimates when applied to individual fossil species (Konrad, 2008; Roth-Nebelsick et al., 2012) and even modern species (Grein et al., 2013) for which all the biochemical, environmental and anatomical parameters required to initialize the model are known (Konrad et al., 2008; Grein et al., 2013; Roth-Nebelsick et al., 2012). We have also not applied the mechanistic stomatal model of Franks et al. (2014) because it is shown to be highly sensitive to initial parametrization of assimilation rate resulting in ± 500 ppm error in palaeo-pCO_2 estimates (McElwain et al., 2016b). Future work on *Eotrigonobalanus furcinervis* will

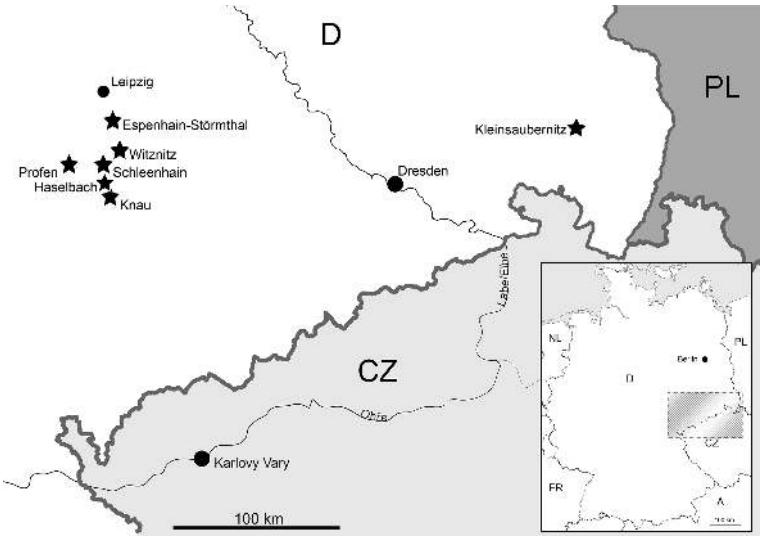

Figure 2. Sites (asterisks) of *Eotrigonobalanus furcinervis*-containing fossil taphocoenoses in central and east Germany considered in the present investigations. Note: the Schleenhain and Haselbach opencast mines revealed taphocoenoses in four and two distinct lithostratigraphic positions respectively (see also stratigraphic chart in Fig. 3). Map legend: D = Germany, CZ = Czech Republic, PL = Poland, FR = France, NL = the Netherlands.

aim to constrain likely palaeo-assimilation rate for this extinct taxon by applying available palaeo-assimilation proxies (McElwain et al., 2016a, b; Wilson et al., 2015) and undertaking elevated pCO_2 experiments on appropriately selected NLEs.

2 Material and methods

2.1 Fossil leaf database

Eotrigonobalanus furcinervis (Rossmässler, 1840; Kvaček and Walther, 1989), an extinct evergreen Fagaceae (Fig. 1), existed from the middle Eocene to the Oligocene–Miocene boundary and was geographically widely distributed, i.e. from central Europe to Russia, as well as to the Mediterranean area (Mai and Walther, 2000; Velitzelos et al., 1999). It is considered as a thermophilous species that grew in evergreen broadleaved forests as well as in mixed mesophytic forests adapted to humid and warm-temperate to subtropical climate (Mai and Walther, 2000). *E. furcinervis* was present in megafossil assemblages or "taphocoenoses" derived from riparian forests, back swamps, peat bogs and zonal vegetation and therefore the parent plant tolerated a wide range of water table conditions and soil characteristics. Whereas in the Eocene it often predominated in zonal Fagaceae–Lauraceae forests (Mai and Walther, 2000), in the Oligocene mixed mesophytic forest it was ecologically subdominant. Based on the combined fossil record of cupules, seeds and leaves, including cuticles, it is commonly accepted that the fossils represent a single long-lived but rather variable fossil species, although minor changes in leaf anatomy have led to the distinction of two subspecies, ssp. *furcinervis* (mainly Eocene, rare in Oligocene) and ssp. *haselbachensis* (only Oligocene; Kvaček and Walther, 1989). The latter is distinguished by the absence of pubescence (trichome clusters) on the abaxial leaf epidermis. Furthermore, a variety of leaf morphotypes can be distinguished that have been interpreted as ecological variants (ecotypes, see Kriegel, 2001).

Except for the material from the Kleinsaubernitz site (Fig. 2), the leaf specimens used here originate from the central German Weißelster Basin (Fig. 2), a coastal alluvial plain at the southern margin of the North German–Polish "Tertiary" Basin (Standke, 2008). This basin is well known for its extensive record of middle Eocene to early Miocene plant assemblages that are mainly derived from azonal vegetation, i.e. riparian and swamp forests (e.g. Mai and Walther, 2000; Kunzmann, 2012). The Knau assemblage represents the fluvial hinterland of the Weißelster lignite swamps (Mai and Walther, 2000).

The leaves used here are derived from a succession of cuticle-rich taphocoenoses that contain *E. furcinervis* ranging in age from the late middle Eocene to the end of the Oligocene (Table 1, Fig. 3). The database analysed here consists of 233 *E. furcinervis* leaf cuticle fragments on as many slides, representing 151 separate individual leaf specimens (Supplement and Table 2). All specimens represent material used in previous taxonomic-systematic studies; they are housed in the Senckenberg Natural History Collections Dresden, Germany. The plant fossil assemblages have been positioned on the most recent lithostratigraphy for central and East Germany (Standke, 2008; Standke et al., 2010; Fig. 3, Table 2) using published information on the fossil sites (Mai and Walther, 1991, 2000; Kunzmann and Walther,

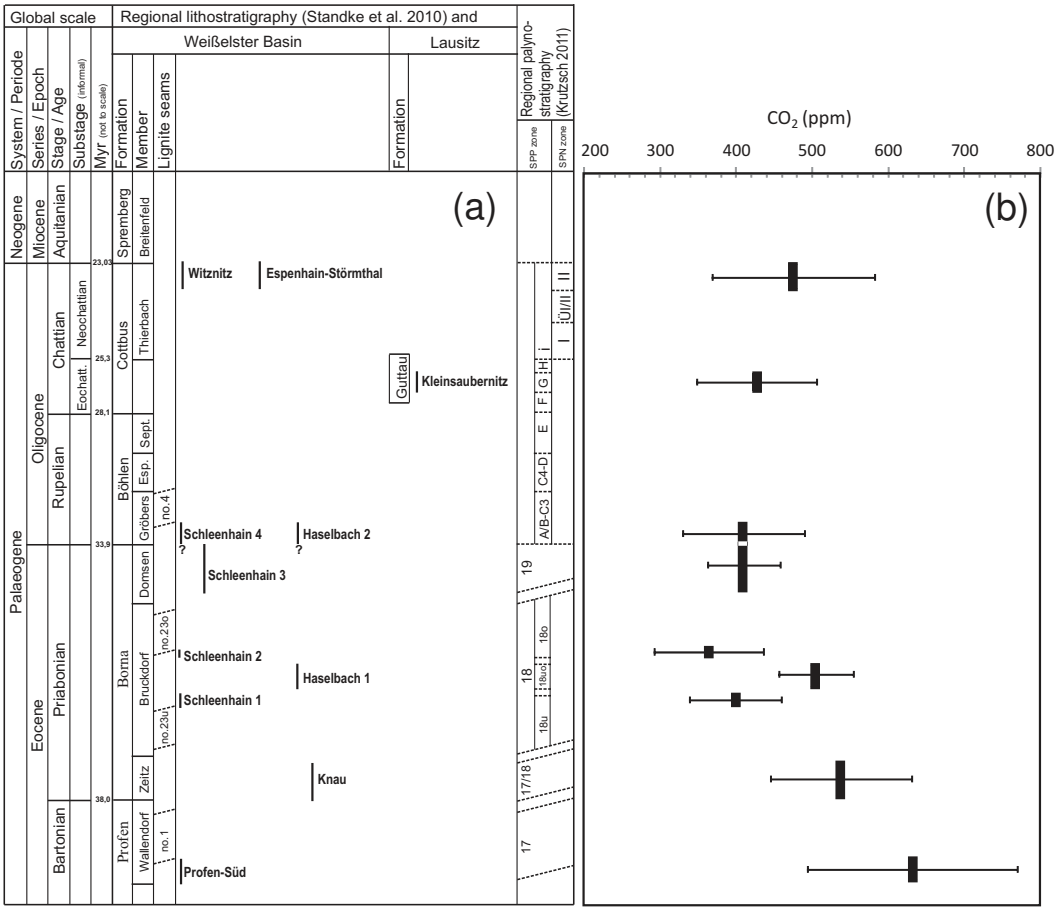

Figure 3. Stratigraphic position of the assemblages with *Eotrigonobalanus furcinervis*, regional lithostratigraphy and Krutzsch's (2011) correlation to the spore-pollen zones including his proposed correlation of spore-pollen zones to global scale (see Sect. 2.2 for explanation and comments on dating uncertainty); black vertical bars next to assemblage names are the temporal uncertainty (based on a combination of lithostratigraphic information of the respective unit and spore-pollen zonation); bars of Schleenhain 1 and 2 are not to scale because gaps in the sediment deposition of the respective units are not equivalent to the duration of spore-pollen zones; gaps between the Eocene spore-pollen (sub-)zones illustrate gaps in the terrestrial sediment record, i.e. erosion. For horizon information see Table 1.

2002; Hennig and Kunzmann, 2013; Ferdani, 2014) and personal observations (LK). Information on dating is provided in Sect. 2.2.

One late Oligocene locality, Kleinsaubernitz (Figs. 2 and 3a), lies within the Lausitz Basin, at its southern margin or even in the hinterland (Standke, 2008). Leaf specimens derive from a sediment-filled maar, volcanic in origin, preserving a parautochthonous assemblage mainly representing zonal vegetation (Walther, 1999) in contrast to the mainly azonal vegetation from the coastal plains of the Weißelster Basin.

2.2 Stratigraphy and dating

The relative stratigraphic positions for the samples from the Weißelster Basin (Figs. 2 and 3a) are based on accumulating knowledge from more than 150 years of geological-palaeontological investigations of the respective units – see Walther and Kunzmann (2008) for a summary. The samples are derived from a superposed sequence of four lignite seams and their associated strata (Table 1, Fig. 3a), the subdivisions of which can be readily recognized across different opencast mines.

It is not possible to directly correlate the plant-fossil-bearing horizons in the Weißelster Basin to the global marine stratigraphy. Although there are a number of brackish-marine intercalations (Standke et al., 2010) most of these strata lack fossils suitable for biostratigraphy. As is typical for lignite-bearing non-consolidated sedimentary successions (i.e. gravel, sands, silts, clays) hard parts of mineralized organisms that might be used for biostratigraphy in continental sequences (such as mammals and charophytes) are lacking due to dissolution by humic acids originating from organic material. Non-consolidated sediments do not reveal any casts or moulds of these former fossils. This is also the case for any intercalation of brackish-marine sediments in

Table 1. Lithostratigraphic and phytostratigraphic positions of the *Eotrigonobalanus furcinervis*-containing fossil taphocoenoses in the Weißelster Basin (central Germany); lithostratigraphy after Standke et al. (2010), spore-pollen zonation after Krutzsch (2011).

Assemblage/ site	Reference for fossil flora	Formation	Member	Horizon	Epoch	Spore-pollen zone
Witznitz	Mai and Walther (1991)	Cottbus	Thierbach	Witznitz	end of Oligocene	II
Espenhain-Störmthal	Mai and Walther (1991)	Cottbus	Thierbach	Witznitz	end of Oligocene	II
Haselbach 2	Mai and Walther (1978)	Böhlen	Gröbers	Haselbach	earliest Oligocene?	20A/B
Schleenhain 4	Kunzmann and Walther (2012)	Böhlen	Gröbers	Haselbach	earliest Oligocene?	20A/B
Schleenhain 3	Kunzmann and Walther (2002)	Borna	Domsen	overlying bed of lignite seam 23o	latest Eocene	19 (?)
Schleenhain 2	Ferdani (2014), Mai and Walther (2000)	Borna	Bruckdorf	underlying bed of lignite seam 23o and leaf measure in lignite seam 23o	late Eocene	18o
Haselbach 1	Mai and Walther (2000)	Borna	Bruckdorf	intercalated bed between lignite seam 23u and 23o	late Eocene	18uo
Schleenhain 1	Hennig and Kunzmann (2013)	Borna	Bruckdorf	overlying bed of lignite seam 23u	late Eocene	18u
Knau	Mai and Walther (2000)	Borna	uncertain	fluvial deposit	late Eocene	17/18
Profen-Süd	Fischer in Mai and Walther (2000)	Profen	Wallendorf	underlying bed of lignite seam 1	late middle Eocene	17

the Weißelster Basin profile. The lack of common index fossils prevents accurate stratigraphic chronology in the basin and reduces the level of stratigraphic resolution compared with that typically attainable for marine deposits (e.g. Roth-Nebelsick et al., 2014). Furthermore, heterogeneity in facies types (channel, floodplain, tidal deposits, swamps) and in grain sizes of the sediments precludes the use of magnetostratigraphic methods which need longer sequences of fine-grained sediments without facies shifts (e.g. lake sediments) to produce reliable data.

Based on a series of consecutive pollen assemblages in the Weißelster Basin strata a regional phytostratigraphic concept was developed (Krutzsch, 1967) that can be applied to all formations, members and submembers, and also to all lignite seams and even individual seam measures (Krutzsch, 2011). All of our investigated material is unambiguously assigned to a certain unit of the regional lithostratigraphic scheme (Fig. 3a) and thus connected to a respective pollen zone or subzone (Fig. 3a, Table 1). However, the pollen zonation yields only a relative age for a given horizon within the regional palynostratigraphic framework and does not enable correlation to global stratigraphy or to the global timescale. The attempt by Krutzsch (2011) to correlate the Eocene spore-pollen zones with the global timescale is used herein (Fig. 3a) as it is the only available information to interpret our assemblages. A "late" Eocene age (i.e. late Bartonian + Priabonian, Krutzsch 2011) for our respective assemblages has been previously inferred based on floristic comparison to assemblages from the nearby Bohemian basins (Czech Republic) some of which have absolute dates from volcanic rocks (i.e. Kučlin, Staré Sedlo, Roudníky; Kvaček et al., 2014).

In the younger part of the succession, marine deposits have yielded index fossils suitable for biostratigraphy. Marine strata above the Gröbers Member of the Böhlen Formation are placed into regional dinoflagellate zones D13 and D14 (Köthe, 2005; Standke et al., 2010) which are Rupelian in age. The Haselbach horizon of the Gröbers Mem-

Table 2. The Saxony *Eotrigonobalanus furcinervis* database, including spore-pollen zones (Krutzsch, 2011) and epoch inferred from them, stomatal density counts and pCO_2 calibration results, all shown with standard deviation, average pCO_2 in bold. Comparison to previously published stomatal proxy-based pCO_2 results from central Germany and nearby regions listed in the far right column.

Sites	Epoch	Spore/ pollen zone	SD (stomata mm^{-2})	pCO_2 min (ppm)	pCO_2 max (ppm)	pCO_2 average (ppm)	No. of leaves	Other studies CO_2 ppm
Witznitz, Espenhain-Störmthal	latest Oligocene	II	569.02 ± 108.40	351.6 ± 79.12	600.02 ± 135.03	475.81 ± 107.08	45	~420 to ~530 ppm[1]
Kleinsaubernitz	late Oligocene	20G	623.29 ± 97.82	316.8 ± 58.41	540.71 ± 99.7	428.76 ± 79.05	25	~400 ppm[1]
Schleenhain 4, Haselbach 2	earliest Oligocene (?)	20 A/B	657.13 ± 118.98	302.5 ± 59.31	516.29 ± 101.23	409.40 ± 80.27	21	n/a
Schleenhain 3	latest Eocene	19	642.88 ± 84.05	303.1 ± 35.54	517.24 ± 60.66	410.17 ± 48.10	11	n/a
Schleenhain 2	late Eocene	18o	740.65 ± 148.90	269.56 ± 53.01	460.05 ± 90.48	364.80 ± 71.74	39	n/a
Haselbach 1	late Eocene	18uo	505.88 ± 47.06	373.50 ± 35.99	637.45 ± 61.43	505.48 ± 48.72	2	~470 (ave.)[2] ~270 (min)[2] ~710 (max)[2]
Schleenhain 1	late Eocene	18u	661.18 ± 90.93	296.15 ± 44.65	505.43 ± 76.206	400.79 ± 60.429	4	n/a
Knau	late Eocene	17/18	495.50 ± 77.80	397.33 ± 68.7	678.12 ± 117.25	537.73 ± 92.98	4	n/a
Profen-Süd	late middle Eocene	17	426.14 ± 83.56	467.87 ± 101.78	798.51 ± 173.71	633.19 ± 137.74	1	~470 (ave.)[2] ~270 (min)[2] ~710 (max)[2]

[1] Applying the Konrad et al. (2008) stomatal optimization model in a multispecies consensus approach (Grein et al., 2013). [2] Applying the Konrad et al. (2008) stomatal optimization model to stratigraphically lumped *Eotrigonobalanus furcinervis* samples from Profen and Haselbach (Roth-Nebelsick et al., 2012). n/a = individual site CO_2 data not reported so direct comparison not possible.

ber, including our assemblage sites Schleenhain 4 and Haselbach 2 (Figs. 2 and 3a), was therefore interpreted to be basalmost Oligocene (Standke et al., 2010; Krutzsch, 2011). However, the only definitive information from the dinoflagellate data is that the samples must be older than mid-Rupelian. Lithofacies changes in the centre of the Weißelster Basin, i.e. the profile in the Schleenhain mine (Kunzmann and Walther, 2002), that indicate major sea level changes below the sample horizon of sites Schleenhain 4 and Haselbach 2 are consistent with those that occur around the Eocene–Oligocene boundary and are documented in other European successions (e.g. Hooker et al., 2009). A basalmost Oligocene age for the Schleenhain 4 and Haselbach 2 sites is also indicated by the first occurrence of *Boehlensipollis hohlii* in the sampled horizon which places the sample in spore-pollen zone 20A/B sensu Krutzsch (2011). *Boehlensipollis hohlii* is regarded as a key element for the Oligocene in central and East Germany (Krutzsch, 2011) and had also been treated as such in the International Geological Correlation Programme (Vinken, 1988). However, it should be mentioned that Collinson (1992) reported several occurrences of the species in the late Eocene of the UK and Frederiksen (1980) reported the species ranging from late middle Eocene to Oligocene in the USA. Possibly the species arose in the USA and spread later via the UK into central Europe but further work is needed to securely link the occurrences of *Boehlensipollis hohlii* with the marine biostratigraphy and the global timescale. In short, there are two independent pieces of evidence (lithofacies, first appearance of *Boehlensipollis hohlii*) that clearly suggest an early Oligocene age for the Schleenhain 4 and Haselbach 2 samples. However, this is not conclusive evidence and direct linkage to the global marine scale is currently not available. The site at Kleinsaubernitz has been located on Fig. 3 based on its pollen assemblage which is zone 20G (Goth et al., 2003).

In summary, the material from the Weißelster Basin comes from a superposed sequence where relative stratigraphic position is securely known (Table 1). Relative changes of SD (and thus pCO_2) through the succession can be placed in context of the spore-pollen zonation. However, the positions of the Eocene–Oligocene boundary and the Oligocene-Miocene boundary cannot be located with certainty in the Weißelster profiles. All age estimates in Figs. 3 and 4 are based on Krutzsch's (2011) proposed correlation of the regional spore-pollen zones to global sea level changes. Independent support is needed for these proposals so they should be regarded as preliminary age information.

2.3 Stomatal density quantification

Cuticles were prepared at the Senckenberg Natural History Collections Dresden as a part of an existing collection. Cuticle slides were prepared using standard methods for Palaeogene material. Fragments removed from leaf specimens with preparation needles were macerated for 1–4 min

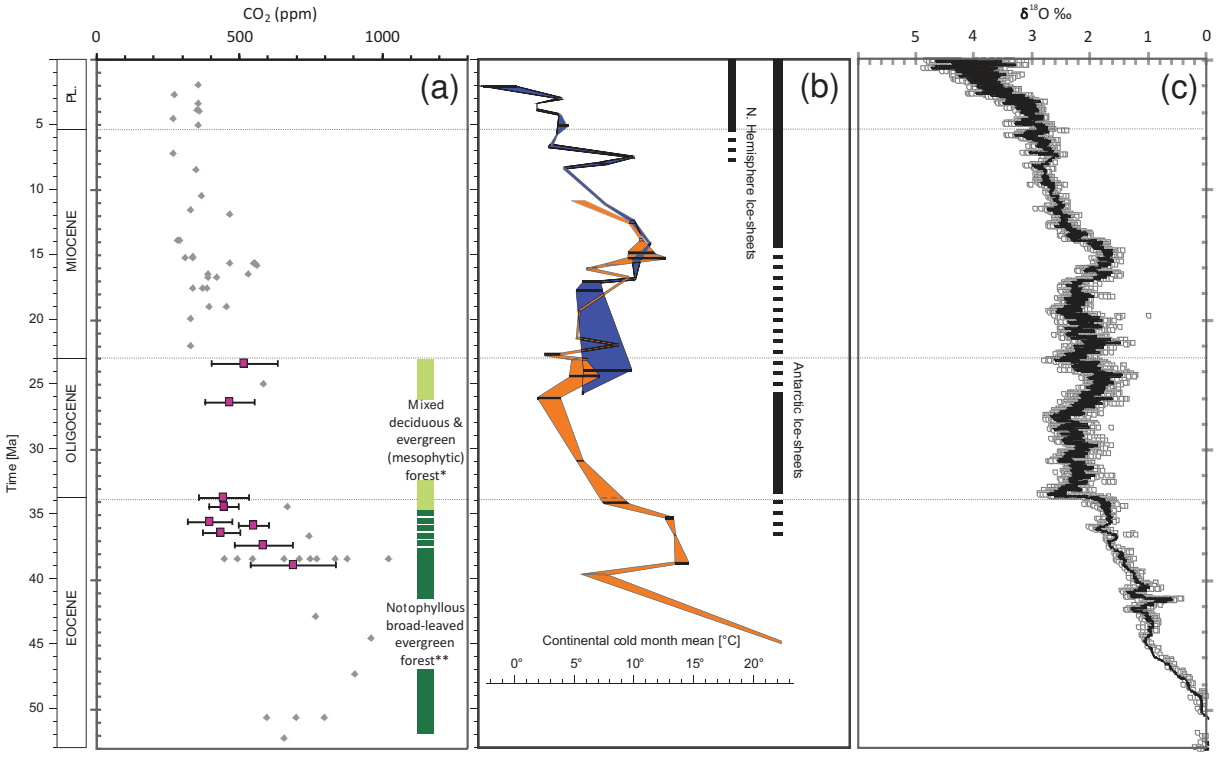

Figure 4. CO_2, vegetation and climate trends through the Cenozoic. The most significant changes in pCO_2, forest ecosystem composition **(a)** and continental climate as tracked by terrestrial plants **(b)** take place in the late Eocene, whereas the most significant change in global temperatures as tracked by marine isotopes **(c)** takes place at the Eocene–Oligocene boundary, indicating that the significant climate transition at the Eocene–Oligocene boundary was preceded by a gradual decrease in pCO_2 during the late Eocene. **(a)** pCO_2 estimates from fossil stomata (this study pink with black error bars) in the context of existing stomatal proxy estimates (in grey from Beerling and Royer, 2011) in a chronostratigraphic framework. Vertical bar shows the gradual late Eocene vegetational restructuring of the dominantly evergreen forests of the Weißelster and North Bohemian basins studied here (dark green to light green), suggesting a potential causal role of pCO_2 decline in the changing ecological forest composition (* Kunzmann and Walther, 2012; ** Kvaček et al., 2014; Kunzmann et al., 2015). Note that the assigned ages for CO_2 values from this study are estimated based on the biostratigraphic controls presented in Fig. 3. Absolute ages were not available for any of the nine fossil study sites (Table 2) although clear superposition information is available throughout allowing good estimates of the temporal sequence of CO_2 estimates (see Fig. 3). **(b)** Continental temperature curve: record of continental cold month mean temperature for central Europe during the last 45 My, redrawn from Mosbrugger et al. (2005). Horizontal bars represent coexistence intervals. Orange curve shows data from the Weißelster and Lausitz Basins, northeast Germany; blue curve shows data from the Lower Rhine Basin, northwest Germany (see Mosbrugger et al. (2005) for details). **(c)** Global climate (temperature) curve derived from stacked records of deep-sea benthic foraminiferal oxygen-isotopes: a proxy for relative changes in marine temperature in the late Eocene prior to ice build up, based on updated records from Deep Sea Drilling Project and Ocean Drilling Program sites. Raw data is smoothed by using 15-point running mean, to minimize biases introduced by uneven temporal and spatial distribution of records – data from Zachos et al. (2001, 2008) and references therein.

in Schulze's solution. Cuticles were then neutralized with NH_4OH, washed with distilled water, and upper and lower cuticles were separated using preparation needles. Finally, the cuticles were stained with Safranin and affixed to slides by glycerol jelly. For this study, the slides were examined microscopically by an adaptation of the methodology set out by Poole and Kürschner (1999) in order to determine SD. According to this protocol, counts from mid-lamina are preferable in establishing SD, but the fragmented nature of a proportion of the fossil material did not allow establishing where individual cuticle samples were located on the original leaf surface (see Fig. 1b). Individual epidermal cells were not easily discernible in the majority of the *E. furcinervis* material, making SI determination impossible. SD was obtained using a Nikon SK Light Microscope at $\times 200$ magnification with a graticule providing a counting field of 0.042 mm^2. The graticule was centred over areas where stomata occurred in greatest numbers (away from veins and margins where those were known, sensu Poole and Kürschner, 1999) and up to five individual counts were recorded for each slide, resulting in 659 SD counts for the database of 151 leaf specimens (Table 1 and Supplement). Data were stored in Microsoft Excel 2010 before being statistically manipulated using MINITAB (version 16.1.1 for Windows).

2.4 Choice of nearest living equivalent and palaeo-pCO_2 calibration

Eotrigonobalanus furcinervis belongs to the Fagaceae, but its phylogenetic position is not well defined. Based on cupule morphology, *Eotrigonobalanus* belongs to a basal clade of the family, exhibiting intermediate characters between modern *Trigonobalanus* and *Castanopsis* (Mai, 1995). However, leaf venation and leaf cuticle micromorphology place *Eotrigonobalanus* with *Trigonobalanus* and *Lithocarpus*, away from *Castanopsis* (Kvaček and Walther, 1989), an affiliation recently confirmed by Denk et al. (2012). Since the phylogeny of Fagaceae has changed considerably (Manos et al., 2001, 2008), an improved systematic framework is still required to confirm the phylogenetic position of *Eotrigonobalanus*. Because the exact relationship of *Eotrigonobalanus* to crown group Fagaceae is unknown, a single nearest living relative (NLR) could not be obtained, hence the nearest living equivalent (NLE) approach has been used for the stomatal proxy-based pCO_2 reconstruction.

In this study, *Trigonobalanus doichangensis* was chosen as the NLE, due to it being a basal species within the Fagaceae family and having leaf macro-morphological and leaf cuticle micro-morphological similarities with *E. furcinervis*, including cyclocytic stomata and similarly structured trichomes (Kvaček and Walther, 1989; see also Denk et al., 2012). Two herbarium specimens of *T. diochangensis*, formerly collected in 1988, were sampled at the Kew Herbarium (Royal Botanical Gardens, Kew, Richmond, Surrey, UK). Approximately 1 cm^2 was cut from mid-lamina of each leaf specimen and dry mounted onto a slide. Five cuticle images from each slide were taken at 200× magnification using a Leica DM2500 epifluorescent microscope with Leica DFC300FX camera (Leica® 312 Microsystems, Wetzlar, Germany) and Syncroscopy Automontage (Syncroscopy Ltd, Cambridge, UK) digital imaging software. A 0.09 mm^2 square was superimposed on each image and stomatal density was determined within this square following the protocol of Poole and Kürschner (1999). SD was determined to be 546.11 mm^2 at pCO_2 of 351 ppm (collection year levels according to NOAA ESRL data, available at http://www.esrl.noaa.gov).

Using the stomatal ratio method with *T. doichangensis* NLE for *E. furcinervis*, we calibrated palaeo-pCO_2 using the equations below to derive minimum and maximum palaeo-pCO_2 ("Modern" and "Carboniferous" Standardization of McElwain and Chaloner, 1995), respectively:

$$\text{Palaeo-}pCO_{2\text{min}}\ (\text{ppm}) = ((\text{SD}_{\text{NLE}} = 546.11)/\text{SD}_{\text{fossil}}) \cdot 351\,\text{ppm}$$

$$\text{Palaeo-}pCO_{2\text{max}}\ (\text{ppm}) = ((\text{SD}_{\text{NLE}} = 546.11)/\text{SD}_{\text{fossil}}) \cdot 600\,\text{ppm}.$$

3 Results

Stomatal density and palaeo-pCO_2 estimates

SD of *E. furcinervis* range between ca. 425 and 740 stomata mm^{-2}. The lowest SD values (signifying highest pCO_2) are found in the oldest deposits, late middle to earliest late Eocene (spore-pollen zone 17), and the highest values (signifying lowest pCO_2) are found in the later late Eocene (spore-pollen zone 18o), representing the most pronounced SD change during the time period covered by the data set (Table 2, Fig. 3b), with three intermediate samples showing intermediate values (spore-pollen zones 17/18, 18u, 18uo). During this interval SD increases by > 300 stomata mm^{-2} or by ca. 75 %, a very significant change indicating a sizeable decrease in pCO_2 in perhaps ca. 3.5 million years. Stomatal densities then decrease slightly again and remain around 600–650 mm^{-2} in the latest Eocene and in samples that may be earliest Oligocene as well as in the late Oligocene (spore-pollen zones 19, 20A/B, 20G, II). At the end of the Oligocene, SD decreases again to ca. 570 mm^{-2}.

Palaeo-pCO_2 calibrated using the stomatal densities of *E. furcinervis* will be discussed as average values and evaluated in terms of relative change, as introduced above. The largest change in palaeo-pCO_2 is the decrease from the late middle to earliest late Eocene of > 250 ppm, from ca. 630 to ca. 365 ppm – a decrease in pCO_2 of ca. 40 % (Fig. 3b; Table 2). Concentrations of CO_2 then increase again by ca. 45 to ca. 410 ppm in the latest Eocene and possibly earliest Oligocene, and further to between ca. 430–475 ppm in the late and latest Oligocene (Fig. 3b; Table 2).

4 Discussion

4.1 Fidelity of the Saxony stomatal pCO_2 record

The Saxony fossil leaf database is unique in that this relatively large database derives from a well-constrained stratigraphic succession and consists of a single species throughout – *E. furcinervis* – which is the most ideal situation when using fossil leaf material to reconstruct palaeo-pCO_2, since inter-species variability is eliminated and stomatal responses to pCO_2 are likely to be consistent through time. The procurement of a single-species data set from multiple stratigraphic levels across several million years is not common, in particular when the stratigraphy represents time intervals of significant climate and/or environmental change, as is the case here. The principal challenge concerning the Saxony stomatal density record was translating the stomatal signal into reliable levels of pCO_2. One of the main limitations associated with the use of palaeo-proxies is the preservational state of fossil material and in this case the preservation of fossil leaves did not allow palaeo-pCO_2 reconstruction using gas exchange models for independent comparison of the

results using the stomatal ratio method because stomatal pore length could not be measured in all samples with confidence. Additionally, there is a lack of available transfer functions for potential NLEs of *E. furcinervis*, so it was not possible either to obtain independent pCO_2 reconstructions using the transfer function method. The stomatal ratio method has however been shown to closely match results produced with transfer function methods (Beerling and Royer, 2002; Royer, 2003; Barclay et al., 2010; Steinthorsdottir et al., 2011b) and is seen as a good alternative where detailed estimates of other photosynthetic parameters, which are required to initialize mechanistic models, are not readily available (McElwain, unpublished data).

The absence of an obvious NLE for *E. furcinervis* – an extinct species of uncertain phylogenetic affinity – further introduces potential errors in pCO_2 calibration. Although we consider *T. doichangensis* the best available NLE, there is no guarantee that its stomatal density and degree of response to pCO_2 closely mirrors that of its distant fossil relative. The pCO_2 levels calibrated here appear somewhat low compared to most previously published pCO_2 data sets, although broadly comparable to stomatal pCO_2 records (Fig. 4a). When testing three additional potentially suitable NLE species for reconstructing pCO_2 using the Saxony database (*Trigonobalanus verticillata, Castanopsis cuspidata* and *Lithocarpus henryi*), the resulting palaeo-pCO_2 values were extremely low – considerably lower than when using the chosen NLE *T. doichangensis* – in many cases being lower than minimum pCO_2 levels required to maintain sufficient plant growth and reproduction (i.e. below the ecological compensation point). This indicates that, for some reason (e.g. species-specific responses) the stomatal proxy-derived pCO_2 estimates presented here based on *E. furcinervis* may be artificially low.

4.2 Comparison with vegetation and proxy continental climate records

Palaeoclimate reconstructions based on central European megafloras reveal a sharp decline in continental cold month mean temperature (Mosbrugger et al., 2005) and mean annual temperature (Moraweck et al., 2015; Kvaček et al., 2014) in the late Eocene (Fig. 4b) which is consistent with the timing of the pCO_2 decline that we report here (Fig. 4a and b), and with global sea surface temperature trends as recorded by marine oxygen-isotopes (Fig. 4c). The marine isotope curve also shows a gradual decrease of temperatures in the late Eocene, but in contrast with the terrestrial records, the most pronounced and abrupt change coincides with the Eocene–Oligocene boundary (Fig. 4c), suggesting that pCO_2 drawdown may have taken place gradually before the slow feedback ice sheet growth was initiated and global temperatures dropped suddenly in response. The possibility remains that future terrestrial proxy reconstructions of pCO_2 will record a transient major drawdown of pCO_2 at the Eocene–Oligocene boundary. In order to resolve this, more proxy records from well-constrained early Oligocene sites must be added.

Furthermore, palaeo-vegetation analysis of the Weißelster and North Bohemian basins reveals that gradual restructuring of dominantly evergreen forests by immigration of deciduous species such as *Platanus neptuni, Trigonobalanopsis rhamnoides* and *Taxodium dubium* (Kunzmann et al. 2015) took place in the late Bartonian to early Priabonian interval around ca. 38 Ma (Kvaček, 2010; Teodoridis and Kvaček, 2015). The temporal coincidence of pCO_2 decline and major vegetation transition – from angiosperm-dominated notophyllous evergreen forests to mixed mesophytic forests – suggests a potential causal role of pCO_2 decline in the changing ecological composition of forests. It may have been in part triggered by differential responses of evergreen and deciduous taxa to declining pCO_2 (Fig. 4a and b), explaining the lag between "temperatures" indicated by terrestrial vegetation and sea surface temperatures recorded by marine oxygen-isotopes (Fig. 4c). The functional trait of deciduousness is an adaptation to episodic cooling (Zanne et al., 2014). However, it has also been demonstrated experimentally (McElwain et al., 2016b) and on theoretical grounds (Niinemets et al., 2011) that taxa with low leaf mass per area or LMA (i.e. those that are deciduous or herbaceous) and high stomatal conductance have faster photosynthetic rates than evergreens at lower atmospheric pCO_2. In contrast, evergreens have higher responsiveness in terms of photosynthetic rates at elevated pCO_2 (Niinemets et al., 2011). A transition from elevated to lower CO_2 atmospheres would therefore favour the ecophysiology of deciduous or low-LMA taxa over evergreen high-LMA species. Further experimental investigation is now required to tease apart the relative importance of "CO_2 starvation" and increased temperature seasonality on the late Bartonian to early Priabonian vegetation transition.

4.3 Comparison with other pCO_2 records

Previously published stomatal proxy-based pCO_2 records from the part of the Cenozoic relevant to this paper do not always agree, but instead report highly elevated (McElwain, 1998; Doria et al., 2011; Grein et al., 2011; Smith et al., 2010), intermediate (Retallack, 2009) or similar to modern (Royer et al., 2001) pCO_2 for the Eocene. Similarly high variability in estimated pCO_2 levels exists for the Oligocene as well as the Miocene (Grein et al., 2013; Kürschner et al., 2008; Roth-Nebelsick et al., 2014; Royer et al., 2001). The results reported here are the highest stratigraphic resolution pCO_2 estimates derived from the late Eocene to early Miocene basins in Saxony (see Table 2, Figs. 1 and 3). Previous studies have tended to only report temporal trends on stomatal parameters (Roth-Nebelsick et al., 2004) or to lump pCO_2 estimates from single Saxony localities into coarse temporal bins making cross comparison difficult (Roth-Nebelsick et al., 2012). However, where indi-

vidual site pCO_2 data are reported (Grein et al., 2013) our estimates are in very good agreement with previous studies despite differences in species and calibration approach (Table 2). For example, Grein et al. (2013) report pCO_2 estimates of ∼ 400 ppm and between ∼ 430 and ∼ 530 ppm respectively for the sites Kleinsaubernitz and Witznitz (Fig. 3) using the Konrad et al. (2008) stomatal optimization model in a consensus approach on multiple species (3–4) including *E. furcinervis* (Table 2). The optimization model produces a very large range of pCO_2 estimates however (∼ 270 to 710 ppm), when applied to *E. furcinervis* alone from stratigraphically lumped samples from Haselbach and Profen (Table 2) (Roth-Nebelsick et al., 2012). In comparison with the study of Roth-Nebelsick et al. (2012), we report seven stratigraphically well-resolved pCO_2 estimates spanning the same interval for which they report a single lumped average (∼ 470 ppm) for two sites (Table 2). This is thus the first study to resolve a significant drop in palaeo-pCO_2 in the late Eocene, prior to the E–O boundary from a stratigraphically well-constrained and relatively high-resolution record.

Using a rigorous generalized statistical framework, Beerling et al. (2009) revised previously published pCO_2 estimates based on *Ginkgo* and *Metasequoia* from the early Eocene and middle Miocene upwards by 150–250 ppm. Based on this revision, average stomatal proxy-based pCO_2 is 450–700 ppm in the Palaeogene and 500–600 ppm in the Neogene (Beerling et al., 2009). Interestingly, the younger set of pCO_2 estimates was fully compatible to marine proxy data and modelling results (e.g. Pagani et al., 2005; Hansen et al., 2008), whereas the older set of estimates seemed to underestimate pCO_2 compared to the other approaches, even after the upwards revision of stomatal pCO_2 values (see Fig. 4 in Beerling et al., 2009). However, Kürschner et al. (2008) indicated that an upwards correction of 150–200 ppm – a so-called "correction factor" – was necessary also when reconstructing Miocene palaeo-pCO_2 with two species from the Lauraceae family. Recently discrepancies between the various pCO_2 proxies have narrowed significantly, and a coherent pattern of long-term Cenozoic pCO_2 has emerged, indicating pCO_2 mostly in the hundreds rather than thousands of ppm, although shorter-term inter-proxy discrepancies remain (see Beerling and Royer, 2011, Fig. 1). It has thus become evident that pCO_2 values reconstructed using the stomatal proxy do not require a correction factor.

Pearson et al. (2009) reconstructed pCO_2 for the late Eocene to early Oligocene using the planktonic foraminifera boron isotope pH proxy and found that the main reduction in pCO_2 took place before the main phase of EOT ice growth (ca. 33.6 Ma: DeConto et al., 2008), followed by a sharp recovery to pre-transition levels and then a more gradual decline. Their results thus support the central role of declining pCO_2 in Antarctic ice sheet initiation and development and agree broadly with carbon cycle modelling (e.g. Merico et al., 2008). The quantitative estimates of pCO_2 varied greatly however, according to which $\delta^{11}B$ value was used to derive pH, with geochemical models of the boron cycle suggesting a range of 37–39 ‰ for sea water (sw) $\delta^{11}B$ during this time (Simon et al., 2006). The range of pCO_2 values spanned from ca. 2000–1500 ppm at the upper end and ca. 620–450 ppm at the lower end (Pearson et al., 2009). Recently published alkenone-based pCO_2 records found significantly declining pCO_2 before, as well as during, the Antarctic glaciation (EOT and earliest Oligocene), supporting the pCO_2 pattern of Pearson et al. (2009) and the role of pCO_2 as the primary forcing agent of Antarctic glaciation, consistent with model-derived thresholds (DeConto et al., 2008; Pagani et al., 2011; Zhang et al., 2013). The alkenone-derived data set values are overall higher – but not much higher – than those derived by stomatal densities, with late Eocene values of ca. 1000 ppm, minimum value of ca. 670 at 33.57 Ma and then gradual decline to ca. 350 ppm at the Oligocene-Miocene boundary.

In general therefore, Cenozoic stomatal proxy-based pCO_2 values, reconstructed using the available methods, tend to report somewhat lower pCO_2 values than alkenone- or boron-based proxies as well as those from mass balance modelling. As discussed above, isotope-based proxy records depend on a range of assumptions that influence the output interpretation to a large extent. In addition, it has recently been shown that the modelled pCO_2 threshold for Antarctic glaciation at the EOT, routinely referred to be ca. 700 ppm (DeConto and Pollard, 2003), is in fact highly dependent on the type of climate model used and the configurations of the model (Gasson et al., 2014), implying that the range of Cenozoic pCO_2 may be due for an update. It is noteworthy that most existing stomatal proxy-based pCO_2 records report a similar range of low pCO_2 values for this time interval and an internally consistent pattern is emerging for the Cenozoic (see Fig. 4a). Stomatal proxy-based pCO_2 records that are independently calibrated using different species/genera and families usually agree with one another and show Eocene–Miocene pCO_2 in the range of 800–300 ppm (Fig. 4a). Although this discrepancy between proxies needs to be better understood before significant reevaluation of the role of pCO_2 in Cenozoic climate change is warranted, it should not be a priori rejected that collectively stomatal proxy records may accurately indicate lower pCO_2 levels during the Cenozoic than previously assumed.

4.4 Implications for Cenozoic climate sensitivity

The concept of Earth's climate sensitivity – usually defined as the equilibrium surface temperature response to doubling of pCO_2 ($2 \times CO_2$) – is a key parameter for understanding the mechanisms of future climate change. Recently there has been much focus on accurately and uniformly defining this concept, but although progress has been made, discrepancies still remain. The term most in use for predicting future climate change is "equilibrium climate sensitivity", defined as the response of global mean surface temperatures to a

$2 \times CO_2$ radiative forcing after all the fast feedbacks have occurred (changes in atmospheric temperatures, clouds, water vapour, winds, snow, sea ice, etc.), but before the slow feedbacks occur (mainly ice sheet, vegetation and the carbon cycle responses) and often estimated to be ca. 3 °C (Rohling et al., 2012; Royer et al., 2012; Hansen et al., 2013; Huber et al., 2014; the Intergovernmental Panel on Climate Change report 2013 best estimate 1.5–4.5 °C). When studying palaeoclimate sensitivity, which has the potential to be accurately inferred from high-resolution palaeo-climate proxy archives, both fast and slow feedbacks must be considered to define a related concept – the "Earth system sensitivity", where e.g. pCO_2 may act both as forcer and as feedback, and which depends to a large degree on the initial climate state (Royer et al., 2007; Hansen et al., 2013). In the Cenozoic, pCO_2 is involved in climate change both as forcing and feedback, with evidence of increased climate sensitivity in warm climates, rather than cool ones (Hansen et al., 2013).

The Eocene–Oligocene global cooling transition is represented by a large increase in deep-sea benthic foraminiferal oxygen isotope values, reflecting simultaneously decrease in temperatures and increased ice sheet growth, with as of yet no proxy to accurately separate the relative effects of the two (Zachos et al., 2001, 2008). Constraining the decrease in temperature that occurred during the transition is thus a work in progress, but consensus is emerging around a ca. 2–5 °C cooling in sea surface as well as mean annual air temperature (e.g. Lear et al., 2009; Zachos et al., 2008; Liu et al., 2009; Bohaty et al., 2012; Wade et al., 2012; Hren et al., 2013; Inglis et al., 2015; Petersen and Schrag, 2015). The EOT cooling and glaciation was forced by a decrease in pCO_2 from ca. 1000 to ca. 600 ppm based on marine isotopes and climate modelling (e.g. DeConto et al., 2008; Pearson et al., 2009; Pagani et al., 2011) or ca. 800 to ca. 400 ppm based on stomatal records (e.g. Beerling and Royer, 2011; this data set) – a decrease of at least ca. 40 % in pCO_2 in < 5 Ma. A simple estimation of Earth system sensitivity during the EOT suggests elevated sensitivity compared to today, implying an enhancing factor by fast and/or slow feedbacks, such as ice sheet growth, but the radiative contribution of each is presently unknown (Lunt et al., 2010; Goldner et al., 2014; Gasson et al., 2014; Maxbauer et al., 2014). The transition in Earth's climate mode from the Eocene greenhouse to the Oligocene icehouse was driven by changes in pCO_2 (and associated feedbacks) that largely fall within the range of modern to predicted future pCO_2 – albeit in the opposite direction. Understanding how the Earth system responds to radiative forcing within this range (i.e. understanding Earth system sensitivity) is of considerable interest, with the input and correlation of multiple palaeo-pCO_2 proxy records being of crucial importance.

5 Conclusions

The new terrestrial stomatal proxy-based pCO_2 record presented here, derived from fossil leaves of *Eotrigonobalanus furcinervis* (extinct Fagaceae, beech tree family) from Saxony, Germany, spans the late middle Eocene to latest Eocene, with two sampling levels which are probably from earliest Oligocene, and two samples from later in the Oligocene. The record indicates that pCO_2 decreased continuously and gradually by ca. 40 % during the late Eocene, from ca. 630 ppm in the late middle Eocene to ca. 365 ppm in the late Eocene and ca. 410 ppm near the Eocene–Oligocene boundary. Late and latest Oligocene pCO_2 was slightly higher at around 430–475 ppm. Although the pCO_2 values reported here may be artificially low, due to factors inherent to stomatal proxy-based calibration, they nonetheless broadly agree with the pCO_2 range of previously published Eocene–Miocene stomatal proxy records, indicating that Cenozoic pCO_2 may have been considerably lower than previously thought based on marine proxies. The substantial late Eocene decrease in pCO_2 reported here is consistent with terrestrial records of vegetation change and reconstructions of coldest month mean temperatures, as well as with marine isotope records of global sea surface temperatures. The substantial drop in temperatures and/or ice sheet growth that defines the Eocene–Oligocene boundary in the marine record is not recorded here. This may be caused by the possibility that the Saxony record does not possess the stratigraphic resolution to record such a change, or indicate that decrease in pCO_2 took place before the recorded decrease in global sea surface temperatures. The results reported here lend strong support to the theory that pCO_2 drawdown, rather than continental reorganization, was the main forcer of the Eocene–Oligocene climate change, when a "tipping point" was reached in the latest Eocene, triggering the plunge of the Earth system into icehouse conditions.

The Supplement related to this article is available online at doi:10.5194/cp-12-439-2016-supplement.

Acknowledgements. M. Steinthorsdottir gratefully acknowledges funding from Stockholm University postdoctoral research fellowship SU 619-2974-12 Nat and the Bolin Centre for Climate Research. J. C. McElwain and A. S. Porter acknowledge funding from Science Foundation Ireland grant SFI 08/RFP/EOB1131 and the European Research Council grant ERC-2011-StG 279962-OXYEVOL. A. Holohan acknowledges funding from the Programme for Research in Third-Level Institutions (PRTLI) – Ireland, and the European Regional Development Fund. MSc student Gael Giraud is acknowledged for early work on the project. Sincere thanks go to Carola Kunzmann and Franziska Ferdani (Dresden) for preparation of cuticle slides of *Eotrigonobalanus furcinervis*; to Zlatko Kvaček (Prague) for numerous discussions on Palaeogene vegetation development; to Karolin Moraweck

(Dresden) for discussions on palaeoclimate estimation in the middle and late Eocene using the Coexistence Approach and for drafting the fossil site map (Fig. 1). The Royal Botanic Gardens Kew Herbarium and the National Botanic Gardens Ireland provided live and herbarium specimens of *Trigonobalanus doichangensis, T. verticillata, Castanopsis cuspidata* and *Lithocarpus henryi*, for analysis and selection of Nearest Living Equivalent for pCO_2 calibration. Finally, Helen Coxall (Stockholm University) and Matthew Huber (University of New Hampshire, USA) are sincerely thanked for constructive criticism on earlier versions of this paper, advice and helpful discussions.

Edited by: Y. Godderis

References

Barclay, R. S., McElwain, J. C., and Sageman, B. B.: Carbon sequestration activated by a volcanic CO_2 pulse during Ocean Anoxic Event 2, Nat. Geosci., 3, 205–208, 2010.

Beerling, D. J. and Royer, D. L.: Reading a CO_2 signal from fossil stomata, New Phytol., 153, 387–397, 2002.

Beerling, D. J. and Royer, D. L.: Convergent Cenozoic CO_2 history, Nat. Geosci., 4, 418–420, 2011.

Beerling, D. J., Fox, A., and Anderson, C. W.: Quantitative uncertainty analyses of ancient atmospheric CO_2 estimates from fossil leaves, Am. J. Sci., 309, 775–787, 2009.

Beerling, D. J., Chaloner, W. G., and Woodward, F. I.: Vegetation-climate-atmosphere interactions: Past, present and future, Philos. T. Roy. Soc. B., 353, 1365, 3-4, 1998.

Bohaty, S. M., Zachos, J. C., and Delaney, M. L.: Foraminiferal Mg/Ca evidence for Southern Ocean cooling across Eocene–Oligocene transition, Earth Planet. Sc. Lett., 317–318, 251–261, 2012.

Brownlee, C.: The long and the short of stomatal density signals, Trends Plant Sci., 6, 441–442, 2001.

Caballero, R. and Huber, M.: State-dependent climate sensitivity in past warm climates and its implications for future climate projections, P. Natl. Acd. Sci. USA, 110, 14162–14167, 2013.

Collinson, M. E.: Vegetational and floristic changes around the Eocene/Oligocene boundary in western and central Europe, in: Eocene–Oligocene climate change and biotic evolution, edited by: Prothero, D. R. and Berggren, W. A., Princeton University Press, Princeton, New Jersey, 437–450, 1992.

Coxall, H. K. and Pearson, P. N.: The Eocene–Oligocene transition, in: Deep-time perspectives on climate change, edited by: Williams, M., Haywood, A. M., Gregory, F. J., and Schmidt, D. N., The Geological Society, London, 351-387, 2007.

Coxall, H. K., Wilson, P. A., Pälike, H., Lear, C. H., and Backman, J.: Rapid stepwise onset of Antarctic glaciation and deeper calcite compensation in the Pacific Ocean, Nature, 433, 53–57, 2005.

DeConto, R. M. and Pollard, D.: Rapid Cenozoic glaciation of Antarctica induced by declining atmospheric CO_2, Nature, 421, 245–249, 2003.

DeConto, R. M., Pollard, D., Wilson, P. A., Pälike, H., Lear, C. H., and Pagani, M.: Thresholds for Cenozoic bipolar glaciation, Nature, 455, 652–656, 2008.

Denk, T., Grímsson, F., and Zetter, R.: Fagaceae from the early Oligocene of Central Europe: Persisting new world and emerging old world biogeographic links, Rev. Palaeobot. Palyno., 169, 7–20, 2012.

Doria, G., Royer, D. L., Wolfe, A. P., Fox, A., Westgate, J. A., and Beerling, D. J.: Declining atmospheric CO_2 during the late middle Eocene climate transition, Am. J. Sci., 311, 63–75, 2011.

Ferdani, F.: Obereozäne Floren aus dem zentralen Weißelsterbecken (Mitteldeutschland) und ihre paläoökologische Position, Altenburger Naturwiss. Forsch., 16, 1–115, 2014.

Finsinger, W. and Wagner-Cremer, F.: Stomatal-based inference models for reconstruction of atmospheric CO_2 concentration: a method assessment using a calibration and validation approach, Holocene, 19, 757–764, 2009.

Foster, G. L., Lear, C. H., and Rae, J. W. B.: The evolution of pCO_2, ice volume and climate during the middle Miocene, Earth Planet. Sc. Lett., 341–344, 243–254, 2012.

Franks, P. J., Royer, D. L., Beerling, D. J., Van de Water, P. K., Cantrill, D. J., Barbour, M. M., and Berry, J. A.: New constraints on atmospheric CO_2 concentration for the Phanerozoic, Geophys. Res. Lett., 41, 4685–4694, 2014.

Frederiksen, N. O.: Mid-Teriary Climate of Southeastern United States: The sporomorph evidence, J. Paleontol., 54, 728–739, 1980.

Frommer, W. B.: COmmon Sense, Science, 327, 275–276, 2010.

Gasson, E., Lunt, D. J., DeConto, R., Goldner, A., Heinemann, M., Huber, M., LeGrande, A. N., Pollard, D., Sagoo, N., Siddall, M., Winguth, A., and Valdes, P. J.: Uncertainties in the modelled CO_2 threshold for Antarctic glaciation, Clim. Past, 10, 451–466, doi:10.5194/cp-10-451-2014, 2014.

Goldner, A., Herold, N., and Huber, M.: Antarctic glaciation caused ocean circulation changes at the Eocene–Oligocene transition, Nature, 511, 574–577, 2014.

Goth, K., Suhr, P., and Schulz, R.: Zwei Forschungsbohrungen in das verdeckte Maar von Baruth (Sachsen), Z. Angew. Geol., 49, 9–17, 2003.

Gray, J. E., Holroyd, G. H., van der Lee, F. M., Bahrami, A. R., Sijmons, P. C., Woodward, F. I., Schuch, W., and Heterington, A. M.: The HIC signalling pathway links CO_2 perception to stomatal development, Nature, 408, 713–716, 2000.

Greenwood, D. R., Scarr, M. J., and Christophel, D. C.: Leaf stomatal frequency in the Australian tropical rainforest tree *Neolitsea dealbata* (Lauraceae) as a proxy measure of atmospheric pCO_2, Palaeogeogr. Palaeocl., 196, 375–393, 2003.

Grein, M., Konrad, W., Wilde, V., Utescher, T., and Roth-Nebelsick, A: Reconstruction of atmospheric CO_2 during the early middle Eocene by application of a gas exchange model to fossil plants from the Messel Formation, Germany, Palaeogeogr. Palaeocl., 309, 383–391, 2011.

Grein, M., Oehm, C., Konrad, W., Utescher, T., Kunzmann, L., and Roth-Nebelsick, A.: Atmospheric CO_2 from the late Oligcene to early Miocene based on photosynthesis data and fossil leaf characteristics, Palaeogeogr. Palaeocl., 374, 41–51, 2013.

Hansen, J., Sato, M., Kharecha, P., Beerlib, D. J., Berner, R. A., Masson-Delmotte, V., Pagani, M., Raymo, M., Royer, D. L., and Zachos, J. C.: Target atmospheric CO_2: Where should humanity aim?, Open. Atmos. Sci. J., 2, 217–231, 2008.

Hansen, J., Sato, M., Russell, G., and Kharecha, P.: Climate sensitivity, sea level and atmospheric carbon dioxide, Philos. T. Roy. Soc. A, 371, 20120294, doi:10.1098/rsta.2012.0294, 2013.

Hennig, D. and Kunzmann, L.: Taphonomy and vegetational analysis of a late Eocene flora from Schleenhain (Saxony, Germany), Geol. Saxon., 59, 75–88, 2013.

Hooker, J. J., Grimes, S. T., Mattey, D. P., Collinson, M. E., and Sheldon, N. D.: Refined correlation of the UK Late Eocene-Early Oligocene Solent Group and timing of its climate history, in: The Late Eocene Earth–Hothouse, Icehouse, and Impacts, edited by: Koeberl, C. and Montanari, A., Geological Society of America Special Paper 452, Geological Society of America, 179–195, 2009.

Hren, M. T., Sheldon, M. D., Grimes, S. T., Collinson, M. E., Hooker, J. J., Bugler, M., and Lohman, K. C.: Terrestrial cooling in Northern Europe during the Eocene–Oligocene transition, P. Natl. Acd. Sci. USA, 110, 7562–7567, 2013.

Hu, H., Boisson-Dernier, A., Israelsson-Nordström, M., Böhmer, M., Xue, A., Ries, A., Godoski, J., Kuhn, J. M., and Schroeder, J. I.: Carbonic anhydrases are upstream regulators of CO_2-controlled stomatal movements in guard cells, Nat. Cell Biol., 12, 87–93, 2010.

Huber, M. and Caballero, R.: The early Eocene equable climate problem revisited, Clim. Past, 7, 603–633, doi:10.5194/cp-7-603-2011, 2011.

Huber, M., Beyerle, U., and Knutti, R.: Estimating climate sensitivity and future tempereature in the resence of natural climate variability, Geophys. Res. Lett., 41, 2086–2092, 2014.

Inglis, G. N., Farnsworth, A., Lunt, D., Foster, G. L., Hollis, C. J., Pagani, M., Jardine, P. N., Pearson, P. N., Markwick, P., Galsworthy, A. M. J., Raynham, L., Taylor, K. W. R., and Pancost, R. D.: Descent towards the Icehouse: Eocene sea surface cooling inferred from GDGT distributions, Paleoceanography, 30, 1000–1020, doi:10.1002/2014PA002723, 2015.

IPCC Climate Change 2007: The Physical Science Basis, in: Contribution of Working Group I to the Fourth Assessment Report of the Intergovernmental Panel on Climate Change, edited by: Solomon, S., Qin, D., Manning, M., Chen, Z.,Marquis, M., Averyt, K. B., Tignor M., and Miller, H. L., Cambridge University Press, Cambridge, UK and New York, NY, USA, 2007.

Konrad, W., Roth-Nebelsick, A., and Grein, M.: Modelling of stomatal density response to atmospheric CO_2, J. Theor. Biol., 253, 638–658, 2008.

Köthe, A.: Korrelation der Dinozysten-Zonen mit anderen biostratigraphisch wichtigen Zonierungen im Tertiär Norddeutschlands, Rev. Paléobiol., 24, 697–718, 2005.

Kriegel, K.: Untersuchung der Blattmorphologie und Blattanatomie von *Eotrigonobalanus furcinervis* (Rossmäßler) Walther & Kvaček und seine Vergesellschaftung mit anderen teriären Sippen vom Mitteleozän bis Oligo-/Miozän Mitteleuropas, Unpubl. Diploma thesis, Technical University Dresden, Dresden, 93 pp., 2001.

Krutzsch, W.: Der Florenwechsel im Alttertiär Mitteleuropas auf Grund von sporenpaläontologischen Untersuchungen, Abh. Zentr. Geol. Inst., 10, 17–37, 1967.

Krutzsch, W.: Stratigrafie und Klima des Palaogens im Mitteldeutschen Astuar im Vergleich zur marinen nordlichen Umrahmung, Z. Dt. Ges. Geowiss., 162, 19–46, 2011.

Kunzmann, L.: Early Oligocene plant taphacoenosis with mass occurrnce of *Zingiberiodeophyllum* (extinct Zingiberales) from central Germany, Palaios, 27, 765–778, 2012.

Kunzmann, L. and Walther, H.: Eine obereozäne Blätterflora aus dem mitteldeutschen Weißelster-Becken, Paläont. Z., 76, 261–282, 2002.

Kunzmann, L. and Walther, H.: Early Oligocene plant taphocoenoses of the Haselbach megafloral complex and the reconstruction of palaeovegetation, Palaeobiol. Palaeoenviron., 92, 295–307, 2012.

Kunzmann, L., Kvaček, Z., Teodoridis, V., Müller, C., and Moraweck, K.: Vegetation dynamics of riparian forest in central Europe during the late Eocene, Palaeontographica B, in press, 2015.

Kürschner, W. M., Kvaček, Z., and Dilcher, D. L.: The impact of Miocene atmospheric carbon dioxide fluctuations on climate and the evolution of terrestrial ecosystems, P. Natl. Acd. Sci. USA, 105, 449–453, 2008.

Kvaček, Z.: Forest flora and vegetation of the European early Palaeogene – a review, Bull. Geosci., 85, 63–76, 2010.

Kvaček, Z. and Walther, H.: Revision der mitteleuropa ischen Fagaceen nach blattepidermalen Charakteristiken: Teil III. T. *Dryophyllum* DEBEY ex SAPORTA und Eotrigonobalanus WALTHER and KVAČEK, Feddes Repertorium, 100, 575–601, 1989.

Kvaček, Z., Teodoridis, V., Mach, K., Přikryl, T., and Dvořák, Z.: Tracing the Eocene–Oligocene transition: a case study from North Bohemia, Bull. Geosci., 89, 21–66, 2014.

Lake, J. A., Woodward, F. I., and Quick, W. P.: Long-distance CO_2 signalling in plants, J. Exp. Bot., 53, 183–193, 2002.

Lear, C. H., Bailey, T. R., Pearson, P. N., Coxall, H. K., and Rosenthal, Y.: Cooling and ice growth across the Eocene–Oligocene transition, Geology, 36, 251–254, 2009.

Liu, X.-Y., Gao, Q., Han, M., and Jin, J.-H.: The pCO_2 estimates of the late Eocene in South China based on stomatal densities of *Nageia* Gaertner leaves, Clim. Past. Discuss., 11, 2615–2647, doi:10.5194/cpd-11-2615-2015, 2015.

Liu, Z., Pagani, M., Zinniker, D., DeConto, R., Huber, M., Brinkhuis, H., Shah, S. R., Leckie, R. M., and Pearson, A.: Global cooing during the Eocene–Oligocene climate transition, Science, 27, 1187–1190, 2009.

Lunt, D. J., Valdes, P. J., Dunkley Jones, T., Ridgwell, A., Haywood, A. M., Schmidt, D. N., Marsh, R., and Maslin, M.: CO_2-driven ocean circulation changes as an amplifier of Paleocene-Eocene thermal maximum hydrate destabilization, Geology, 38, 875–878, 2010.

Mai, D. H.: Tertiäre Vegetationsgeschichte Europas, Methoden und Ergebnisse, G. Fischre, Jena, 691 pp., 1995.

Mai, D. H. and Walther, H.: Die Floren der Haselbacher Serie im Weißelster-Becken (Bezirk Leipzig, DDR), Abh. Staatl. Mus. Mineral. Geol. Dresden, 28, 1–101, 1978.

Mai, D. H. and Walther, H.: Die oligozänen und untermiozänen Floren Nordwest-Sachsens und des Bitterfelder Raumes, Abh. Staatl. Mus. Mineral. Geol. Dresden, 38, 1–230, 1991.

Mai, D. H. and Walther, H.: Die Fundstellen eozäner Floren NW-Sachsens und des Bitterfelder Raumes, Altenburger Naturwiss. Forsch., 33, 3–59, 2000.

Manos, P. S., Zhou, Z.-K., and Cannon, C. H.: Systematics of Fagaceae: Phylogenetic Tests of Reproductive Trait Evolution, Int. J. Plant Sci., 162, 1361–1379, 2001.

Manos, P. S., Cannon, C. H., and Oh, S.-H.: Phylogenetic Relationships and Taxonomic Status Of the Paleoendemic Fagaceae

Of Western North America, Recognition Of A New Genus, *Notholithocarpus*, Madroño, 55, 181–190, 2008.

Maxbauer, D. P., Royer, D. L., and LePage, B. A.: High Arctic forests during the middle Eocene supported by moderate levels of atmospheric CO_2, Geology, 42, 1027–1030, 2014.

McElwain, J. C.: Do fossil plants reflect palaeoatmospheric CO_2 concentration in the geological past?, Philos. T. Roy. Soc. B, 353, 83–96, 1998.

McElwain, J. C. and Chaloner, W. G.: Stomatal density and index of fossil plants track atmospheric carbon dioxide in the Palaeozoic, Ann. Bot.-Lond., 76, 389–395, 1995.

McElwain, J. C., Montañez, I., White, J. D., Wilson, J. P., and Yiotis, C.: Was atmospheric CO_2 capped at 1000 ppm over the past 300 million years?, Palaeogeogr. Palaeocl., 441, 653–658, doi:10.1016/j.palaeo.2015.10.017, 2016a.

McElwain, J. C., Yiotis, C., and Lawson, T.: Using modern plant trait relationships between observed and theoretical maximum stomatal conductance and vein density to examine patterns of plant macroevolution, New Phytol., 209, 94–103, doi:10.1111/nph.13579, 2016b.

Merico, A., Tyrrell, T., and Wilson, P. A.: Eocene/Oligocene ocean de-acidification linked to Antarctic glaciation by sea-level fall, Nature, 452, 979–982, 2008.

Moraweck, K., Uhl, D., and Kunzmann, L.: Estimation of late Eocene (Bartonian-Priabonian) terrestrial palaeoclimate: contributions from megafloral assemblages from central Germany, Palaeogeogr. Palaeocl., 433, 247–258, 2015.

Mosbrugger, V., Utescher, T., and Dilcher, D. L.: Cenozoic continental climatic evolution of Central Europe, P. Natl. Acd. Sci. USA, 102, 14964–14969, 2005.

Niinemets, Ü., Flexas, J., and Peñuelas, J.: Evergreens favored by higher responsiveness to increased CO_2, Trends Ecol. Evol., 26, 136–142, 2011.

Pagani, M., Zachos, J. C., Freeman, K. H., Tipple, B., and Bohaty, S.: Marked Decline in Atmospheric Carbon Dioxide Concentrations During the Paleogene, Science, 309, 600–603, 2005.

Pagani, M., Huber, M., Liu, Z., Bohaty, S. M., Henderiks, J., Sijp, W., Krishnan, S., and DeConto, R. M.: The role of carbon dioxide during the onset of Antarctic glaciation, Science, 334, 1261–1264, 2011.

Pearson, P. N., Foster, G. L., and Wade, B. S.: Atmospheric carbon dioxide through the Eocene–Oligocene climate transition, Nature, 461, 1110–1114, 2009.

Petersen, S. V. and Schrag, D. P.: Antarctic ice growth before and after the Eocene–Oligocene transition: New estimates from clumped isotope paleothermometry, Paleoceanography, 30, 1305–1317, 2015.

Pollard, D. and DeConto, R. M.: Hysteresis in Cenozoic Antarctic ice-sheet variations, Global Planet. Change, 45, 9–21, 2005.

Poole, I. and Kürschner, W. M.: Stomatal density and index: the practice, in: Fossil plants and spores: modern techniques, edited by: Jones, T. P. and Rowe, N. P., The Geological Society, London, 257–260, 1999.

Prothero, D. R.: The late Eocene–Oligocene extinctions, Annu. Rev. Earth Planet. Sc. Lett., 22, 145–165, 1994.

Retallack, G. J.: A 300-million-year record of atmospheric CO_2 from fossil plant cuticles, Nature, 411, 287–290, 2001.

Retallack, G. J.: Greenhouse crises of the past 300 million years, Geol. Soc. Am. Bull., 121, 1441–1455, 2009.

Rohling, E. J., Sluijs, A., Dijkstra, H. A., Köhler, P., van de Wal, R. S. W., von der Heydt, A. S., Beerling, D. J., Berger, A., Bijl, P. K., Crucifix, M., DeConto, R., Drifhout, S. S., Federov, A., Foster, G. L., Ganapolski, A., Hansen, J., Hönisch, B., Hooghiemstra, H., Huber, M., Huybers, P., Knutti, R., Lea, D. W., Lourens, L. J., Lunt, D., Masson-Demotte, V., Medina-Elizalde, M., Otto-Bliesner, B., Pagani, M., Pälike, H., Renssen, H., Royer, D. L., Siddall, M., Valdes, P., Zachos, J. C., and Zeebe, R. E. (PALAEOSENS project members): Making sense of palaeoclimate sensitivity, Nature, 491, 683–691, 2012.

Rossmässler, E. A.: Die Versteinerungen des Braunkohlensandsteines aus der Gegend von Altsattel in Böhmen (Ellbogener Kreis), Arnoldsche Buchhandl., Dresden, Leipzig, 42 pp., 1840.

Roth-Nebelsick, A., Utescher, T., Mosbrugger, V., Diester-Haass, L., and Walther, H.: Changes in atmospheric CO_2 concentrations and climate from the Late Eocene to Early Miocene: Palaeobotanical reconstruction based on fossil floras from Saxony, Germany, Palaeogeogr. Palaeocl., 205, 43–67, 2004.

Roth-Nebelsick, A., Grein, M., Utescher, T., and Konrad, W.: Stomatal pore length change in leaves of *Eotrigonolanalus furcinervis* (Fagaceae) from the Late Eocene to the Latest Oligocene and its impact on gas exchange, Rev. Palaeobot. Palynol., 174, 106–112, 2012.

Roth-Nebelsick, A., Oehm, C., Grein, M., Utescher, T., Kunzmann, L., Friedrich, J. P., and Konrad, W.: Stomatal density and index data of *Platanus neptuni* leaf fossils and their evaluation as a CO_2 proxy for the Oligocene, Rev. Palaeobot. Palynol., 206, 1–9, 2014.

Royer, D. L.: Stomatal density and stomatal index as indicators of paleoatmospheric CO_2 concentration, Rev. Palaeobot. Palynol., 114, 1–28, 2001.

Royer, D. L.: Estimating latest Cretaceous and Tertiary atmospheric CO_2 concentration from stomatal indices, in: Causes and consequences of globally warm climates in the early Paleogene, GSA Special Papers 369, edited by: Wing, S. L., Gingerich, P. D., Schmitz, B., and Thomas, E., Geological Society of America, 79–93, doi:10.1130/0-8137-2369-8.79, 2003.

Royer, D. L., Wing, S. L., Beerling, D. J., Jolley, D. W., Koch, P. L., Hickey, L. J., and Berner, R. A.: Paleobotanical evidence for near present-day levels of atmospheric CO_2 during part of the tertiary, Science, 292, 2310–2313, 2001.

Royer, D. L., Berner, R. A., and Park, J.: Climate sensitivity constrained by CO_2 concentrations over the past 420 million years, Nature, 446, 530–532, 2007.

Royer, D. L., Pagani, M., and Beerling, D. J.: Geobiological constraints on Earth system sensitivity to CO_2 during the Cretaceous and Cenozoic, Geobiology, 10, 298–310, 2012.

Rundgren, M. and Björck, S.: Late-glacial and early Holocene variations in atmospheric CO_2 concentration indicated by high-resolution stomatal index data, Earth Planet. Sc. Lett., 213, 191–204, 2003.

Sheldon, N. D., Mitchell, R. L., Collinson, M. E., and Hooker, J. J.: Eocene–Oligocene transition paleoclimatic and paleoenvironmental record from the Isle of Wight (UK), in: The Late Eocene Earth: Hothouse, Icehouse, and Impacts, GSA Special Papers 452, edited by: Koeberl, C. and Montanari, A., Geological Society of America, 249–259, 2009.

Simon, L., Lécuyer, C., Maréchal, C., and Coltice, N.: Modelling the geochemical cycle of boron: Implications for the long-term

δ^{13}B evolution of seawater and oceanic crust, Chem. Geol., 225, 61–76, 2006.

Smith, R. Y., Greenwood, D. R., and Basinger, J. F.: Estimating paleoatmospheric pCO_2 during the Early Eocene Climatic Optimum from stomatal frequency of *Ginkgo*, Okanagan Highlands, British Columbia, Canada, Palaeogeogr. Palaeocl., 293, 120–131, 2010.

Sloan, L. C. and Barron, E.: "Equable" climates during Earth history, Geology, 18, 489–492, 1992.

Standke, G.: Tertiär, in: Geologie von Sachsen. Geologischer Bau und Entwicklungsgeschichte, edited by: Pälchen, W. and Walther, H., 358-419, E. Schweizerbart'sche Verlagsbuchhandlung, Stuttgart, 2008.

Standke, G., Escher, D., Fischer, J., and Rascher, J.: Das Tertiär Nordwestsachsens. Ein geologischer Überblick, Sächsisches Landesamt für Umwelt, Landwirtschaft und Geologie, Freiberg/Saxony, 157 pp., 2010.

Steinthorsdottir, M. and Vajda, V.: Early Jurassic (late Pliensbachian) CO_2 concentrations based on stomatal analysis of fossil conifer leaves from eastern Australia, Gondwana Res., 27, 932–939, 2015.

Steinthorsdottir, M., Bacon, K. L., Popa, M. E., Bochner, L., and McElwain, J. C.: Bennettitalean leaf cuticle fragments (here *Anomozamites* and *Pterophyllum*) can be used interchangeably in stomatal frequency-based palaeo-CO_2 reconstructions, Palaeontology, 54, 867–882, 2011a.

Steinthorsdottir, M., Jeram, A. J., and McElwain, J. C.: Extremely elevated CO_2 at the Triassic-Jurassic boundary, Palaeogeogr. Palaeocl., 308, 418–432, 2011b.

Steinthorsdottir, M., Wohlfarth, B., Kylander, M., Blaauw, M., and Reimer, P.: Stomatal proxy record of CO_2 concentrations from the last termination suggests an important role for CO_2 at climate change transitions, Quaternary Sci. Rev., 68, 43–58, 2013.

Teodoridis, V. and Kvaček, Z.: Palaeoenvironmental evaluation of Cainozoic plant assemblages from the Bohemian Massif (Czech Republic) and adjacent Germany, Bull. Geosci., 90, 695–720, 2015.

Velitzelos, E., Kvaček, Z., and Walther, H.: Erster Nachweis von *Eotrigonobalanus furcinervis* (Rossm.) Walther and Kvaček (Fagaceae), in Griechenland, Feddes Repertorium, 110, 349–358, 1999.

Vinken, R.: The Northwest European Tertiary Basin. Results of the International Geological Correlation Programme Project No. 124, Geol. Jahrbuch A, 100, 7–508, 1988.

Wade, B. S., Houben, A. J. P., Quaijtaal, W., Schouten, S., Rosenthal., Y., Miller, K. G., Katz, M. E., Wright, J. D., and Brinkhuis, H.: Multiproxy record of abrupt sea-surface coolong across the Eocene–Oligocene transition in the Gulf of Mexico, Geology, 40, 159–162, 2012.

Walther, H.: Die Tertiärflora von Kleinsaubernitz bei Bautzen, Palaeontographica B, 249, 63–174, 1999.

Walther, H. and Kunzmann, L.: Zur Geschichte der paläobotanischen Forschung im Weißelsterbecken, Z. Dt. Ges. Geowiss., 159, 13–21, 2008.

Wilson, J. P., White, J. D., DiMichele, W. A., Hren, M. T., Poulsen, C. J., McElwain, J. C., and Montañez, I. P.: Reconstructing extinct plant water use for understanding vegetation-climate feedbacks: Methods, synthesis and a case study using the Paleozoic era medullosan seed ferns, The Palaeontological Society Papers 21, 167–195, 2015.

Woodward, F. I.: Stomatal numbers are sensitive to increases in CO_2 from pre-industrial levels, Nature, 372, 617–618, 1987.

Wynn, N. G.: Towards a physically based model of CO_2-induced stomatal frequency response, New Phytol., 157, 394–398, 2003.

Zachos, J. C. and Kump, L. R.: Carbon cycle feedbacks and the initiation of Antarctic glaciation in the earliest Oligocene, Global Planet. Change, 47, 51–66, 2005.

Zachos, J. C., Pagani, M., Sloan, L., Thomas, E., and Billups, K.: Trends, rhythms, and aberrations in global climate 65 Ma to present, Science, 292, 686–693, 2001.

Zachos, J. C., Dickens, G. R., and Zeebe, R. E.: An early Cenozoic perspective on greenhouse warming and carbon-cycle dynamics, Nature, 451, 279–283, 2008.

Zanne, A. E., Tank, D. C., Cornwell, W. K., Eastman, J. M., Smith, S. A., FitzJohn, R. G., McGlinn, D. J., O'Meara, B. C., Moles, A. T., Reich, P. B., Royer, D. L., Solties, D. E., Stevens, P. F., Westboy, M., Wright, I. J., Aarssen, L., Bertin, R. I., Calaminus, A., Govaerts, R., Hemmings, F., Leishman, M. R., Oleskyn, J., Soltis, P. S., Swenson, N. G., Warman, L., and Beaulieu, J. M.: Three keys to the radiation of angiosperms into freezing environments, Nature, 506, 89–92, 2014.

Zhang, Y. G., Pagani, M., Liu, Z., Bohaty, S. M., and DeConto, R.: A 40-million-year history of atmospheric CO_2, Philos. T. Roy. Soc. A, 371, 1–20, 2013.